

A Prototype Rattleback Model – a Lie-Poisson Bianchi Type VI System with Chirality

Z Yoshida¹, T Tokieda², and P J Morrison³

¹ Graduate School of Frontier Sciences, University of Tokyo, Kashiwa, Chiba
277-8561, Japan

² Department of Mathematics, Stanford University, Stanford CA 94305-2015, USA

³ Department of Physics and Institute for Fusion Studies, University of Texas at
Austin, TX 78712-1060, USA

E-mail: yoshida@ppl.k.u-tokyo.ac.jp, tokieda@stanford.edu,
morrison@physics.utexas.edu

Abstract. A non-dissipative idealized model of the rattleback is investigated. The model has two first integrals, energy and an intriguing function that was accidentally discovered but had eluded interpretation. Here, the noncanonical three-dimensional Hamiltonian structure for the rattleback model is devised, and shown to be associated with the Bianchi Type VI Lie algebra, which appears for the first time in a concrete physical example. Its Casimir, whose existence is a consequence of the noncanonical Lie-Poisson form, is seen to be the intriguing first integral. The system is integrable on each Casimir surface, and the chirality of the rattleback motion is shown to be caused by the geometric skewness of the symplectic leaf. The Casimir is perturbed by embedding in a larger four-dimensional phase space, in which the system becomes canonical but non-integrable. The perturbed system exhibits chaotic spin reversals, and chirality persists as long as the perturbation is weak enough for the orbit to make chaotic itinerancy among different leaves.

PACS numbers: 45.20.Jj, 47.10.Df, 02.40.Yy

1. Introduction

The rattleback, the elongated asymmetric semi-ellipsoidal top, has amused and bemused scientists and in fact people of all walks of life since ancient times. However, the chirality of this toy, the breaking of mirror symmetry as manifested by rotational preference, points to a serious physical effect that may occur in complicated dynamical systems that describe matter. In order to investigate the essence of this chirality, one can begin with rigid-body equations of motion for the rattleback, which are reminiscent of the partial differential equation that describes the $\alpha\omega$ -dynamo [2] proposed to explain the dynamo action in the earth's core that is responsible for the geomagnetic field. From the rattleback rigid-body equations of motion one can extract a prototypical rattleback system (called here PRS) composed of three first order quadratically coupled differential equations [1], a system that is arguably the simplest model containing the essential features of chiral dynamics. It is the further study of the PRS that is the purpose of the present paper.

Although dissipation plays a role in most investigations of rattleback dynamics, we will see that the ideal no-slip, non-dissipative limit, which yields the PRS, has an intriguing Hamiltonian structure that contains essential elements of the dynamics. This PRS Hamiltonian structure is akin to that of spin systems or Euler's equations for the free rigid body (e.g. [7]), where the Poisson bracket has a nonstandard degenerate form, but retains algebraic properties so as to be a realization of a Lie algebra on phase space functions. This Hamiltonian form has been called noncanonical since it is one in terms of variables that are not canonically conjugate, and a special form of such noncanonical Poisson brackets that are defined by any finite-dimensional Lie algebra are known as a Lie-Poisson brackets (e.g. [3]). Lie-Poisson brackets exist for a variety of systems; for example, the Lie-Poisson bracket for Euler's equations for the rigid body is associated with the Lie algebra $\mathfrak{so}(3)$ and that for the equations describing the Kida vortex of fluid mechanics is associated with the Lie algebra $\mathfrak{so}(2, 1)$ [10]. In fact, these examples represent two of nine three-dimensional real Lie algebras of the Bianchi classification used for homogeneous cosmologies in general relativity (e.g. [8, 9]), by which they are referred to as Type IX and Type VIII, respectively. Remarkably we will see that the PRS corresponds to Type VI_h with $h \neq -1$ of this classification, which to our knowledge is the first time a Lie-Poisson bracket for this rather unfamiliar algebra has been identified for a natural physical system.

A beneficial consequence of the Lie-Poisson construction for these three-dimensional systems is an immediate geometrical characterization of the dynamics. All such Lie-Poisson systems possess two constants of motion: the Hamiltonian as expected and a Casimir invariant that arises from degeneracy of the Poisson bracket. Consequently, all of these systems are integrable and the intersection of the surfaces of the two constants of motion determines the global qualitative nature of the solution. For example, for the free rigid body the Casimir is the angular momentum sphere, and it is elementary that the intersection of this sphere with the energy ellipsoid determines the nature of the

orbits, viz., that rotation about largest and smallest principal axes are stable, while the intermediate axis is unstable. Similarly, for the Kida problem, the Casimir hyperboloid intersecting the energy surface delineates the possible rotational, librational, or unstable dynamics of the Kida vortex patch [10]. Because this common Hamiltonian form occurs for all of the Bianchi types, it occurs for the PRS, and this immediately explains the additional intriguing first integral obtained in [1] – it is the Casimir invariant for Type $VI_{h \neq -1}$. Intersection of the Casimir for the PRS and its Hamiltonian reveals that all three variables of the system perform periodic oscillations, with the spin around the vertical axis reversing sign. The strangeness of the rattleback motion is in a sense a manifestation of the unfamiliarity of the Type $VI_{h \neq -1}$ algebra.

In perturbation theory, we usually perturb the Hamiltonian, the initial conditions, or the physical parameters, etc. Here, unusually, we perturb the dimension of the problem by embedding the three-dimensional system into a larger, 4-dimensional phase space. In so doing we gain canonicity but lose integrability: in fact we observe chaotic reversals of the spin, which may serve as a minimum model for the reversals of the magnetic poles driven by a dynamo. The extended system is described by invoking a method of canonization discussed in [4, 5].

The paper is organized as follows. In section 2 we begin, in section 2.1, by recalling the PRS of [1], followed in section 2.2 by the demonstration that it is a 3-dimensional noncanonical Hamiltonian system. Here we review the Lie-Poisson construction and show the PRS has the Poisson bracket for Type $VI_{h \neq -1}$ and that the extra invariant of [1] is indeed the Casimir invariant for this algebra. Since to our knowledge a complete list of all 3-dimensional Lie-Poisson brackets and their Casimirs does not exist in the literature, we do so in Table 1. In section 3, we analyze the mechanism of chirality from the perspective of Hamiltonian theory. Sections 3.1 and 3.2 are devoted to the spectral analysis of linearized systems; in particular, we show how the singularity of the Lie-Poisson algebra causes chiral spectra. In section 3.3 we canonize the PRS by effecting a Darboux transformation, showing that this system is a one degree-of-freedom Hamiltonian system on the Casimir constraint surface (symplectic leaf). Section 4 begins with section 4.1 where we embed the PRS into a 4-dimensional phase space, thereby breaking the invariance of the Casimir and allowing for chaotic motion, which is studied in section 4.2. In section 5 we conclude our study with a discussion on broader implications of the results. We have included Appendix A, which has an alternative Hamiltonian formulation where the roles of the Hamiltonian and of the Casimir are interchanged; this amounts to a nonlinear deformation of the Bianchi Type IX (i.e. $\mathfrak{so}(3)$) Lie-Poisson algebra; the deformation is scaled by the aspect-ratio parameter λ (corresponding to $-h$ of Type VI) of the rattleback model.

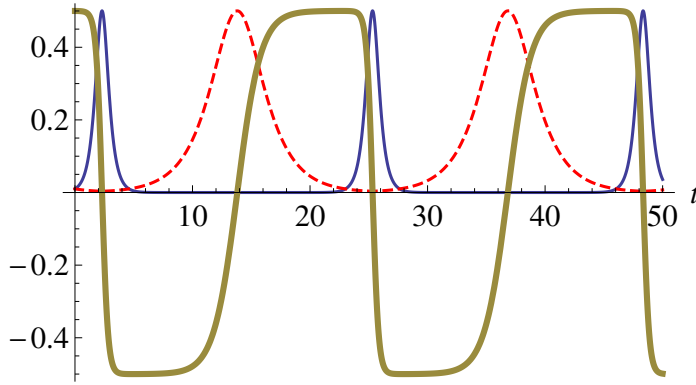


Figure 1. Typical solution of spin reversal (reproduced from Fig. 1 of [1]). $\lambda = 4$, $P(0) = R(0) = 0.01$, $S(0) = 0.5$. The blue curve is pitching (P), the red dotted curve is rolling (R), the brown thick curve is spinning (S).

2. Model equations and Hamiltonian formalism

2.1. Rattleback model

The equations of the PRS are as follows:

$$\frac{d}{dt} \begin{pmatrix} P \\ R \\ S \end{pmatrix} = \begin{pmatrix} R \\ \lambda P \\ 0 \end{pmatrix} \times \begin{pmatrix} P \\ R \\ S \end{pmatrix} = \begin{pmatrix} \lambda PS \\ -RS \\ R^2 - \lambda P^2 \end{pmatrix}. \quad (1)$$

Compared with equation (5.5) of [1], we have adopted a more felicitous notation where P, R, S stand for the *pitching*, *rolling*, and *spinning* modes of the motion. The quantity λ is a positive parameter that encodes the *aspect ratio* of the rattleback.

Figure 1 shows a typical solution of the rattleback model. Note that the common claim that ‘the forward spin is stable whereas the backward spin is unstable’ is in fact false. Both spins are unstable, but the exponents of instability are unequal. We tend not to see the forward spin go into rattling and reverse, merely because the dissipation (friction on the floor) kills the motion before this weak instability kicks in. The backward spin, whose instability is strong, reverses quickly while the motion lasts. In the absence of dissipation the rattleback keeps reversing back and forth, as is easily seen in tabletop experiments. Indeed, thanks to the Hamiltonian structure discussed in section 1 the system (1) is integrable. Examination of the intersection of the Hamiltonian with the Casimir reveals that every orbit is periodic, as will be seen in section 2.2 (cf. Fig. 2). Here we will also see how the two growth rates arise because of a singularity in the Hamiltonian structure.

2.2. Hamiltonian form

Despite the fact that the phase space is odd-dimensional, it is possible, and useful, to cast the equations (1) into Hamiltonian form. In terms of the coordinates $\mathbf{X} =$

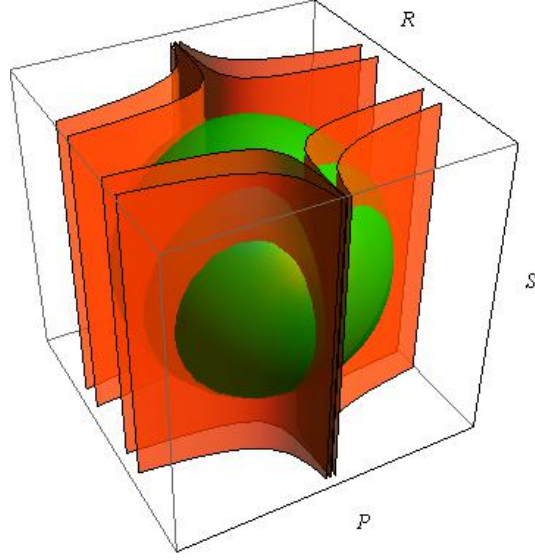


Figure 2. Orbits are the intersections of an energy level $H = \frac{1}{2}(P^2 + R^2 + S^2) = \text{const.}$ (green sphere) and a Casimir surface $C = PR^\lambda = \text{const.}$ (red curved sheet); the leaves $C = 1, 0.1, -0.1, -1$ are shown. The aspect-ratio parameter is taken to be $\lambda = 4$.

$(P \ R \ S)^T \in \Omega \subset \mathbb{R}^3$, define a Poisson matrix

$$J = \begin{pmatrix} 0 & 0 & \lambda P \\ 0 & 0 & -R \\ -\lambda P & R & 0 \end{pmatrix}, \quad (2)$$

and denote by $\langle \cdot, \cdot \rangle_\Omega$ the standard inner product on the phase space Ω . If we take the *Hamiltonian*

$$H = \frac{1}{2} \langle \mathbf{X}, \mathbf{X} \rangle_\Omega = \frac{1}{2} (P^2 + R^2 + S^2), \quad (3)$$

then (1) is cast into the following Hamilton form:

$$\frac{d}{dt} \mathbf{X} = J \partial_{\mathbf{X}} H = \{ \mathbf{X}, H \}_J, \quad (4)$$

where in the second equality the Poisson bracket

$$\{F, G\}_J = \langle \partial_{\mathbf{X}} F, J \partial_{\mathbf{X}} G \rangle_\Omega \quad (5)$$

makes $C^\infty(\Omega)$ into a Poisson algebra, a Lie algebra realization on functions, since it is bilinear, antisymmetric, and can be shown to satisfy the Jacobi identity.

The degeneracy of J yields a *Casimir invariant*

$$C = PR^\lambda, \quad (6)$$

characterized by the property $\{C, G\}_J = 0 \ \forall G \in C^\infty(\Omega)$. Since

$$\det(zI - J) = z(z^2 + \lambda^2 P^2 + R^2),$$

we have $\text{rank} J = 2$ except along the singular set $\lambda^2 P^2 + R^2 = 0$, i.e. $P = R = 0$, where $\text{rank} J$ drops to 0. In this paper we study the dynamics in the regime $\lambda^2 P^2 + R^2 > 0$;

for example it suffices to take the phase space Ω to be an open set in \mathbb{R}^3 on which $|C| = |PR^\lambda|$ is bounded away from 0.

There is a systematic method for constructing Poisson brackets of the form of (5) with (2) given any Lie algebra. Such brackets are called *Lie-Poisson brackets*, because they were known to Lie in the nineteenth century. Let \mathfrak{g} be a Lie algebra with bracket $[\cdot, \cdot]$. Take $\Omega = \mathfrak{g}$ and denote a linear functional on \mathfrak{g} by $\langle \omega, \cdot \rangle \in \mathfrak{g}^*$. Choosing $\omega = \mathbf{X}$ we define, for $F, G \in C^\infty(\Omega)$, $\{F, G\} = \langle \mathbf{X}, [\partial_{\mathbf{X}}F, \partial_{\mathbf{X}}G] \rangle$, where $\partial_{\mathbf{X}}F$ is the gradient in \mathfrak{g} of a function $F(\mathbf{X})$. Because of this construction the Lie-Poisson bracket $\{, \}$ inherits bilinearity, anti-symmetry, and the Jacobi's identity from that of $[\cdot, \cdot]$.

The real three-dimensional Lie algebras can be classified by the scheme used to describe the Bianchi cosmologies, which divides them into nine types. These types of the Bianchi classification (e.g. [8, 9]) are shown in Table 1 along with the associated Casimir invariants, the two-dimensional level sets of which are depicted in Fig.3. We include these here since to our knowledge a complete listing of these Lie-Poisson structures does not appear in this form in the literature. The Bianchi types are divided into two classes: Class A, composed of Types I, II, VI₋₁, VII₀, VIII, and IX, and Class B, composed of Types III, IV, V, VI_{h≠-1}, and VII_{h≠0}. Observe that every Casimir level set for Class B contains a singularity of some kind, while the Casimir level sets for Class A are quadrics and hence regular except for being degenerate at the zero set as, e.g., at the center of the spheres for Type IX. Thus Class A dynamics lives on a two-dimensional symplectic manifold, while Class B dynamics is only locally symplectic.

Examination of Table 1 reveals (upon interchanging the indices 1 and 2 and flipping the sign of 3) that the Poisson matrix of (2) corresponds to a Lie-Poisson bracket of Bianchi Type VI_h, with $h = -\lambda$. The two-dimensional Casimir surfaces are the surfaces $C = PR^\lambda = \text{const}$. At $\lambda = 1$ (Type VI₋₁), the bottom of the contact surface of the rattleback becomes an umbilic (principal curvatures equal), in other words the chirality, as we will see, disappears, so we exclude this case.

3. Chirality from a Hamiltonian perspective

3.1. Regular equilibria and stability

Having identified the PRS with a Lie-Poisson structure, we can immediately apply the energy-Casimir method to determine stability of equilibria (e.g. [3]). Because $\{\mathbf{X}, H\}_J = \{\mathbf{X}, F\}_J$, where $F = H + \mu C$ with μ being a Lagrange multiplier, extremals of F , i.e., $\delta F = 0$, are (relative) equilibrium points. We obtain

$$\frac{\partial F}{\partial P} = P + \mu R^\lambda = 0, \quad \frac{\partial F}{\partial R} = R + \lambda \mu P R^{\lambda-1} = 0, \quad \frac{\partial F}{\partial S} = S = 0, \quad (7)$$

yielding the family of equilibria

$$\mathbf{X}_e^0 = (P_e = C/R_e^\lambda, R_e = \pm(C\sqrt{\lambda})^{\frac{1}{1+\lambda}}, 0),$$

where we have eliminated μ in favor of the value of C . It is easy to show that the above is consistent with $R_e^2 = \lambda P_e^2$, the equilibrium equation obtained from (1). Upon

Table 1. Three-dimensional Lie-Poisson algebras (Bianchi classification). Type I algebra is commutative, so the Poisson bracket is trivial, having three independent Casimirs. To avoid redundancy, for Type IV_h , $h \neq 0, 1$. The Casimir of type $VII_{h \neq 0}$ needs further classification: $h^2 > 4$ gives $C_{VII_{h \neq 0}} = \lambda_- \log(-\lambda_- Z_1 - Z_2) - \lambda_+ \log(\lambda_+ Z_1 + Z_2)$; $h = \pm 2$ gives $C_{VII_{h \neq 0}} = \frac{\pm Z_2}{Z_1 \mp Z_2} + \log(Z_1 \mp Z_2)$; $h^2 < 4$ gives, putting $a = -h/2$ and $\omega = \sqrt{-h^2/4}$ (i.e. $\lambda_{\pm} = a \pm i\omega$), $C_{VII_{h \neq 0}} = 2a \arctan \frac{aZ_1 + Z_2}{\omega Z_1} - \omega \log[(aZ_1 + Z_2)^2 + (\omega Z_1)^2]$.

Type	Poisson matrix	Casimir invariant
I	$J_I = \begin{pmatrix} 0 & 0 & 0 \\ 0 & 0 & 0 \\ 0 & 0 & 0 \end{pmatrix}$	$C_I = \begin{cases} Z_1 \\ Z_2 \\ Z_3 \end{cases}$
II	$J_{II} = \begin{pmatrix} 0 & 0 & 0 \\ 0 & 0 & Z_1 \\ 0 & -Z_1 & 0 \end{pmatrix}$	$C_{II} = Z_1$
III	$J_{III} = \begin{pmatrix} 0 & 0 & Z_1 \\ 0 & 0 & 0 \\ -Z_1 & 0 & 0 \end{pmatrix}$	$C_{III} = Z_2$
IV	$J_{IV} = \begin{pmatrix} 0 & 0 & Z_1 \\ 0 & 0 & Z_1 + Z_2 \\ -Z_1 & -Z_1 - Z_2 & 0 \end{pmatrix}$	$C_{IV} = \frac{Z_2}{Z_1} - \log Z_1$
V	$J_V = \begin{pmatrix} 0 & 0 & Z_1 \\ 0 & 0 & Z_2 \\ -Z_1 & -Z_2 & 0 \end{pmatrix}$	$C_V = \frac{Z_2}{Z_1}$
VI_{-1}	$J_{VI_{-1}} = \begin{pmatrix} 0 & 0 & Z_1 \\ 0 & 0 & -Z_2 \\ -Z_1 & Z_2 & 0 \end{pmatrix}$	$C_{VI_{-1}} = Z_1 Z_2$
$VI_{h \neq -1}$	$J_{VI_{h \neq 0}} = \begin{pmatrix} 0 & 0 & Z_1 \\ 0 & 0 & hZ_2 \\ -Z_1 & -hZ_2 & 0 \end{pmatrix}$	$C_{VI_{h \neq 0}} = \frac{Z_2}{Z_1^h}$
VII_0	$J_{VII_0} = \begin{pmatrix} 0 & 0 & Z_2 \\ 0 & 0 & -Z_1 \\ -Z_2 & Z_1 & 0 \end{pmatrix}$	$C_{VII_0} = Z_1^2 + Z_2^2$
$VII_{h \neq 0}$	$J_{VII_{h \neq 0}} = \begin{pmatrix} 0 & 0 & Z_2 \\ 0 & 0 & -Z_1 + hZ_2 \\ -Z_2 & Z_1 - hZ_2 & 0 \end{pmatrix}$	$C_{VII_{h \neq 0}} = G(Z_1, Z_2, Z_3)$
VIII	$J_{VIII} = \begin{pmatrix} 0 & Z_3 & Z_2 \\ -Z_3 & 0 & -Z_1 \\ -Z_2 & Z_1 & 0 \end{pmatrix}$	$C_{VIII} = Z_1^2 + Z_2^2 - Z_3^2$
IX	$J_{IX} = \begin{pmatrix} 0 & Z_3 & -Z_2 \\ -Z_3 & 0 & Z_1 \\ Z_2 & -Z_1 & 0 \end{pmatrix}$	$C_{IX} = Z_1^2 + Z_2^2 + Z_3^2$

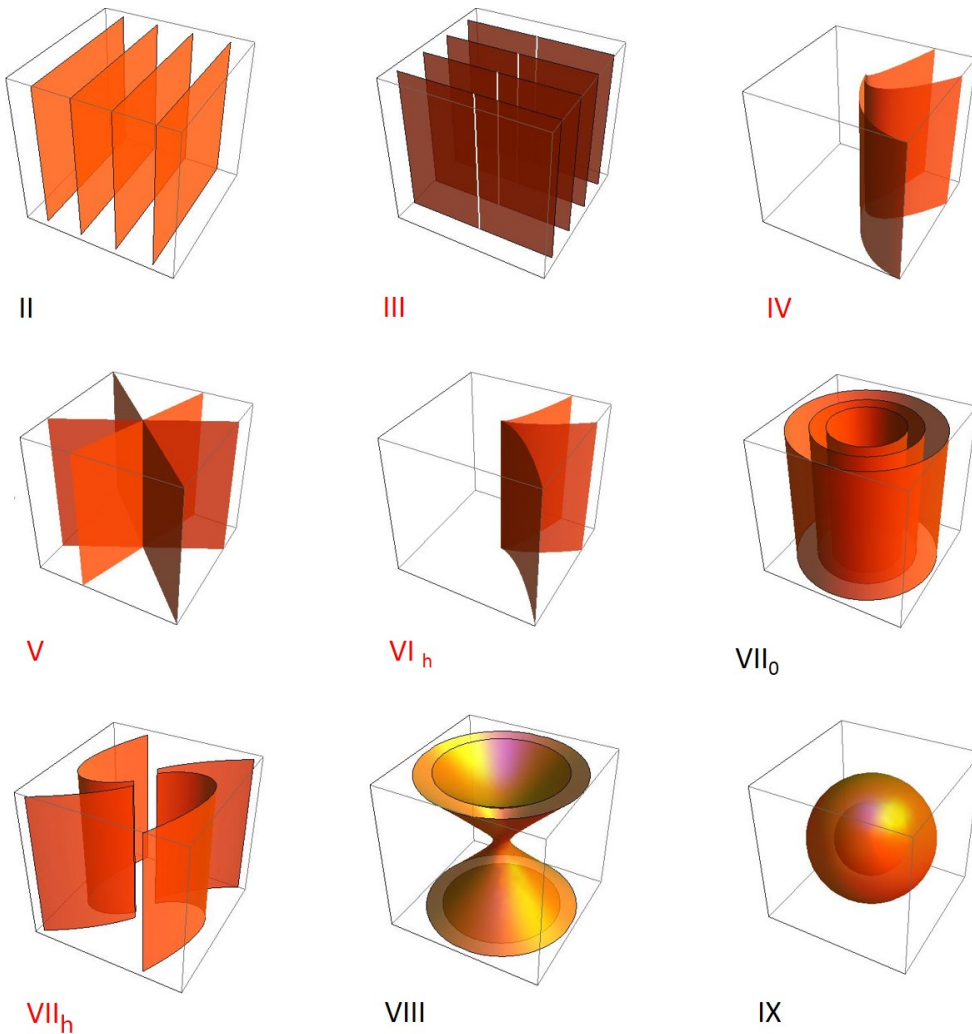


Figure 3. The foliated phase spaces of various Bianchi Lie-Poisson algebras. The leaves are level sets of the Casimirs given in Table 1. Class A, composed of Types I, II, VI_{-1} , VII_0 , VIII, and IX, have regular surfaces (symplectic manifolds), while Class B, composed of Types III, IV, V, $VI_{h \neq -1}$, and $VII_{h \neq 0}$ have singularities. Types II and III are similar, but the latter surfaces are singular along the vertical white lines. The Type VI_h leaves for $h < 0$ are shown in Fig. 2; here those for $h = 1.5$ are shown. The leaves of Type VII_h ($h = 1.5$) are drawn except in the neighborhood of the singularity $Z_1 = Z_2 = 0$. Type II is the Heisenberg algebra, while the Lie-Poisson brackets for Types VIII ($\mathfrak{so}(2, 1)$) and IX ($\mathfrak{so}(3)$), arise for the dynamics of the free rigid body (or spin) and the Kida vortex, respectively. We have associated Type $VI_{h \neq -1}$ with the prototypical rattleback system of (1).

comparison with Fig. 2 we see that for a given value of C there are four points at which the level sets of H and C can be tangent, two for positive values of C and two for negative. Physically this equilibrium corresponds to a periodic rocking motion composed of rolling and pitching, without spin.

Examination of Fig. 2 also reveals that in the vicinity of the four equilibrium points the orbits lie on closed curves. Thus we expect all four equilibrium points to be stable. This can be ascertained by considering the second variation $\delta^2 F$, which measures the energy contained in a perturbation away from an equilibrium point. Setting $P = P_e + \hat{P}$, $R = R_e + \hat{R}$, and $S = \hat{S}$, and expanding to second order yields the Hamiltonian for the linearized dynamics,

$$\begin{aligned} H_L &= \frac{1}{2} \delta^2 F = \frac{1}{2} \left(\hat{P}^2 + \hat{R}^2 + \hat{S}^2 + 2\lambda\mu R_e^{\lambda-1} \hat{R}\hat{P} + \lambda(\lambda-1)\mu R_e^{\lambda-2} P_e \hat{R}^2 \right) \\ &= \frac{1}{2} \left(\hat{P}^2 + \hat{R}^2 + \hat{S}^2 - \frac{2R_e}{P_e} \hat{R}\hat{P} + (1-\lambda) \hat{R}^2 \right). \end{aligned} \quad (8)$$

where the second equality of (8) follows from the equilibrium equations (7).

In terms of H_L linearized equations of motion are given by

$$\frac{d}{dt} \begin{pmatrix} \hat{P} \\ \hat{R} \\ \hat{S} \end{pmatrix} = \begin{pmatrix} 0 & 0 & \lambda P_e \\ 0 & 0 & -R_e \\ -\lambda P_e & R_e & 0 \end{pmatrix} \begin{pmatrix} \partial H_L / \partial \hat{P} \\ \partial H_L / \partial \hat{R} \\ \partial H_L / \partial \hat{S} \end{pmatrix} \quad (9)$$

$$= \begin{pmatrix} 0 & 0 & \lambda P_e \\ 0 & 0 & -R_e \\ -\lambda P_e & R_e & 0 \end{pmatrix} \begin{pmatrix} \hat{P} - \hat{R}R_e/P_e \\ \hat{R} - \hat{P}R_e/P_e + \hat{R}(1-\lambda) \\ \hat{S} \end{pmatrix} \quad (10)$$

$$= \begin{pmatrix} \lambda P_e \hat{S} \\ -R_e \hat{S} \\ 2R_e \hat{R} - 2\lambda P_e \hat{P} \end{pmatrix}. \quad (11)$$

It is easily shown that H_L as given by (8) is not a positive definite quadratic form which would be expected for a stable equilibrium point. However, since the dynamics is constrained to a Casimir leaf, it is necessary to examine the convexity of H_L with variations constrained to the leaf. Such variations were introduced in the context of the energy-Casimir method in [11], where they were called dynamically accessible (*da*) variations (see [3] for review). They are given by using the Poisson matrix to project the variations so as to be tangent to the leaf, as follows:

$$\begin{pmatrix} \hat{P}^{da} \\ \hat{R}^{da} \\ \hat{S}^{da} \end{pmatrix} = \begin{pmatrix} 0 & 0 & \lambda P_e \\ 0 & 0 & -R_e \\ -\lambda P_e & R_e & 0 \end{pmatrix} \begin{pmatrix} g_P \\ g_R \\ g_S \end{pmatrix}, \quad (12)$$

where $\mathbf{g} := (g_P, g_R, g_S)$ are arbitrary. Inserting the *da* variations into H_L yields

$$H_L^{da} = (1+\lambda)R_e^2 g_S^2 + \frac{1}{2}(R_e g_R - \lambda P_e g_P)^2 \quad (13)$$

where use has been made of the equilibrium condition $R_e^2 = \lambda P_e^2$. Because H_L^{da} is positive definite we have stability, which is in agreement with the closed loop orbits seen in Fig. 2 for the intersection of the energy and Casimir surfaces near a point of contact. We also note that a simple eigen-modal analysis gives the frequency of oscillation $\sqrt{2(R_e^2 + \lambda^2 P_e^2)} = |R_e| \sqrt{2(1+\lambda)}$, as well as a zero frequency mode associated with the Casimir invariant [12].

3.2. Chiral spectrum caused by singularity

As previously pointed out, none of the equilibria \mathbf{X}_e^0 possess spin. Yet, it is obvious from (1) that the following are equilibria:

$$\mathbf{X}_e^S = (0, 0, S_e), \quad (14)$$

for any constant value of the spin S_e . These equations occur at a place where the rank of J changes from two to zero and, as addressed in [3], are as a consequence not accessible as extremals of ordinary energy-Casimir variations. However, if we consider δH restricted to da variations, we obtain

$$\delta H^{da} = (\lambda P_e^2 - R_e^2) g_S - \lambda S_e P_e g_P + S_e R_e g_R = 0 \quad (15)$$

which, due to the arbitrariness of \mathbf{g} , gives precisely the vanishing of the right hand side of (1). The investigation of what happens in noncanonical Hamiltonian systems at such rank changing places has been undertaken for both finite and infinite-dimensional systems [4, 5, 6]. Although the Hamiltonian structure has a singularity, the equations of motion (1) are perfectly well-behaved. Linearization about \mathbf{X}_e^S gives the system

$$\frac{d}{dt} \begin{pmatrix} \hat{P} \\ \hat{R} \\ \hat{S} \end{pmatrix} = \begin{pmatrix} \lambda S_e \hat{P} \\ -S_e \hat{R} \\ 0 \end{pmatrix}, \quad (16)$$

which is of special interest for the rattleback dynamics because it addresses the nature of reversal. Assuming $\hat{P}, \hat{R} \sim \exp(\gamma t)$ an eigen-modal analysis of (16) gives the two eigenvalues $\gamma = \lambda S_e$ and $\gamma = -S_e$. Thus, if $S_e > 0$ we have a mode that grows at a rate λS_e , which is faster than one that is damped at S_e . This violation of the symmetry of Hamiltonian spectra is a result of the fact that the rank of the Poisson matrix changes at the position of the equilibrium under study. However, if $S_e < 0$ the growing mode is smaller in absolute value than the damped mode. This asymmetry with the sign of S_e , which was alluded to in section 2.1, was analyzed in [1], where it was concluded that dissipation tends to damp dynamics near $S_e < 0$ because of the smaller growth rate in the nondissipative system. However these growth rates are somewhat an artifact of the peculiar equilibrium-stability analysis. If one starts near an equilibrium point \mathbf{X}_e^0 with small values of P_e and R_e , with an initial condition $S(0) \neq 0$, then the dynamics is accurately described by the intersection of the energy and Casimir surfaces that revealed the periodic motion, both near and far from the equilibrium. We argue in section 3.3 that chirality is best characterized by the asymmetry in the slope of the up and down swings of S during this periodic motion.

3.3. Lie-Darboux canonical form

Because of the Jacobi identity for the noncanonical Poisson matrix of (2), the Lie-Darboux theorem assures that J can be transformed by shifting to coordinates with the Casimir as one coordinate and a canonically conjugate pair that parametrizes the

Casimir leaves as the other two. This transformation takes the Poisson matrix J into the following form:

$$J_{LD} = \begin{pmatrix} 0 & 1 & 0 \\ -1 & 0 & 0 \\ 0 & 0 & 0 \end{pmatrix}. \quad (17)$$

Indeed, under the change of coordinates

$$\mathbf{X} = \begin{pmatrix} P \\ R \\ S \end{pmatrix} \mapsto \mathbf{Z} = \begin{pmatrix} Z_1 \\ Z_2 \\ Z_3 \end{pmatrix} = \begin{pmatrix} \log[R^{-\theta} P^{(1-\theta)/\lambda}] \\ S \\ PR^\lambda \end{pmatrix}, \quad (18)$$

the entries of J_{LD} are given by $\{Z_\mu, Z_\nu\}_J$, where $\{ , \}_J$ is the Poisson bracket (5) expressed in the original coordinates. The zero eigenvalue of J_{LD} corresponds to the Casimir (6). With the choice of $Z_2 = S$, the condition

$$\{Z_1, Z_2\}_J = 1,$$

can be solved to yield Z_1 as in (18), where θ is an arbitrary real parameter. Choosing $\theta = 1$, yields the simpler transformation

$$\mathbf{Z} = \begin{pmatrix} -\log R \\ S \\ PR^\lambda \end{pmatrix}, \quad (19)$$

which has the inverse

$$\mathbf{X} = \begin{pmatrix} Z_3 e^{\lambda Z_1} \\ e^{-Z_1} \\ Z_2 \end{pmatrix}. \quad (20)$$

In terms of the new coordinates, the Hamiltonian (3) takes the form

$$H(\mathbf{Z}) = \frac{1}{2} (Z_3^2 e^{2\lambda Z_1} + e^{-2Z_1} + Z_2^2). \quad (21)$$

If we envision Z_1 as a position variable and $Z_2 = S$ as the corresponding velocity of an oscillator, which is reasonable because $dZ_1/dt = Z_2$ by the equation of motion, then we can rewrite (21) in the intuitive form

$$H(\mathbf{Z}) = \frac{1}{2} Z_2^2 + U_{\lambda,C}(Z_1), \quad (22)$$

where the first term on the right-hand side is a kinetic energy and the remaining terms,

$$U_{\lambda,C}(Z_1) = \frac{1}{2} (e^{-2Z_1} + C^2 e^{2\lambda Z_1}), \quad (23)$$

are a potential energy of the oscillator. Here, both λ and C are constant parameters, the Casimir $C = Z_3$ being determined by the initial condition.

The asymmetric shape of the potential energy $U_{\lambda,C}(Z_1)$ tells a lot about the chirality of the rattleback. As seen in Fig. 4, for $\lambda > 1$ and $C \neq 0$ the family of potentials has gentle slopes toward negative Z_1 and steep cliffs toward positive Z_1 . Suppose we send the rattleback toward positive Z_1 . It runs up a steep potential cliff and sharply reverses

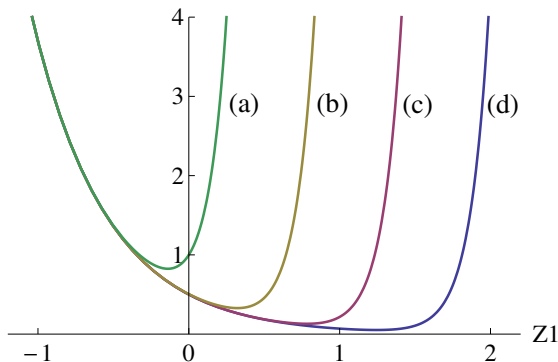


Figure 4. The potential energy $U_{\lambda, C}(Z_1) = \frac{1}{2}(e^{-2Z_1} + C^2 e^{2\lambda Z_1})$ of the canonized equation of motion; $\lambda = 4$, (a) $C = 1$, (b) $C = 0.1$, (c) $C = 0.01$, (d) $C = 0.001$.

the spin, turning $Z_2 = S$ from positive to negative (cf. Fig. 1). As it goes toward negative Z_1 , it trots up a gentle slope and eventually turns from negative to positive Z_2 , but the reversal is not so sharp. When $\lambda < 1$, the asymmetry in the potential is mirrored, and the system acquires an opposite chiral preference, the negative-to-positive turn being sharper than the positive-to-negative turn. The sign of C has no bearing on chirality.

Though we have explained the chiral behavior in terms of the shape of the Hamiltonian (22) in the new coordinates \mathbf{Z} , the root cause of the asymmetry, in the original coordinates $\mathbf{X} = (P R S)^T$, is the *skewness* of the Casimir surface ($C = PR^\lambda = \text{const.}$) against the background of the Hamiltonian (3) symmetric with respect to all the variables. Thus, the chiral dynamics of a rattleback originates from the geometry of the Bianchi Type VI Lie algebra. This is made clear by Fig. 1, the chirality of the rattleback motion is all about the rate of change of the spin S , not about S itself. Therefore, the chirality of the Hamiltonian formalism of Type VI emerges in canonical variables in the term $\partial_{Z_1} H$, where Z_1 is the variable conjugate to $S = Z_2$. Figure 4 shows that H is asymmetric in Z_1 , while it is symmetric in Z_2 .

4. Canonization and unfreezing the Casimir

Integrable Hamiltonian systems like the PRS of section 2 are structurally unstable. Here we perturb this system in a natural way by appending to its canonical Hamiltonian form an additional degree of freedom. This allows us to investigate the ensuing chaos of the PRS.

4.1. Embedding into 4-dimensional phase space

We embed the phase space Ω into a 4-dimensional phase space $\tilde{\Omega}$, and construct an extended Poisson algebra by extending J_{LD} to a cosymplectic matrix \tilde{J}_c . Adjoining a

new coordinate $Z_4 \in \mathbb{R}$, let

$$\tilde{\mathbf{Z}} = \begin{pmatrix} \tilde{Z}_1 \\ \tilde{Z}_2 \\ \tilde{Z}_3 \\ \tilde{Z}_4 \end{pmatrix} = \begin{pmatrix} Z_1 \\ Z_2 \\ Z_3 \\ Z_4 \end{pmatrix} = \begin{pmatrix} -\log R \\ S \\ PR^\lambda \\ Z_4 \end{pmatrix} \in \tilde{\Omega} = \Omega \times \mathbb{R}.$$

The idea of *canonical extension* [4, 5] of J_{LD} is simple: let

$$\tilde{J}_c = \begin{pmatrix} 0 & 1 & 0 & 0 \\ -1 & 0 & 0 & 0 \\ 0 & 0 & 0 & 1 \\ 0 & 0 & -1 & 0 \end{pmatrix}, \quad (24)$$

where the kernel of J_{LD} (the 33 zero corner) gets inflated to a symplectic cell in \tilde{J}_c ; the extended Poisson matrix \tilde{J}_c is the 4×4 cosymplectic matrix, that defines the Poisson algebra $C_{\{\cdot, \cdot\}_{\tilde{J}_c}}^\infty(\tilde{\Omega})$ with the canonical bracket

$$\{F, G\}_{\tilde{J}_c} = \langle \partial_{\tilde{\mathbf{Z}}} F, \tilde{J}_c \partial_{\tilde{\mathbf{Z}}} G \rangle_{\tilde{\Omega}}. \quad (25)$$

As long as the Hamiltonian H does not depend explicitly on the new variable Z_4 , the dynamics on the submanifold Ω is the same as the original dynamics. When this is the case, we call Z_4 a *phantom* variable. Now the invariance of C , which was a hallmark of the degeneracy of J , has been removed: \tilde{J}_c being canonical on the extended phase space $\tilde{\Omega}$ has no Casimir invariant. Instead, C is a first integral coming from the symmetry $\partial_{Z_4} H = 0$ via Noether's theorem.

However, we can *unfreeze* C by perturbing H with a term containing the new variable Z_4 ; in which case, $C = Z_3$ becomes dynamical and Z_4 becomes an *actual* variable. Physically, we may interpret a Casimir as an *adiabatic invariant* associated with an ignorable, small-scale angle variable [4, 5]; upon adjoining Z_4 to H the angle variable materializes from phantom to actual.

4.2. Chaotic chiral dynamics

Let us examine the example

$$H(\tilde{\mathbf{Z}}) = \frac{1}{2} (Z_3^2 e^{2\lambda Z_1} + e^{-2Z_1} + Z_2^2) + \epsilon \frac{1}{2} (Z_3^2 + Z_4^2), \quad (26)$$

where the ϵ term perturbs (21). The perturbation unfreezes the adiabatic invariant $Z_3 = C$. Physically this term represents an oscillation energy.

Figure 5 shows typical solutions of the extended system (24)–(26). In (a) and (b) we plot the orbits projected onto the 3-dimensional $(P R S)$ subspace. Figure 5 (a) depicts an orbit of the original integrable system: this unperturbed case with $\epsilon = 0$ shows the orbit that is the intersection of an energy sphere and a Casimir surface, as was seen in Fig. 2. Figure 5 (b) illustrates a typical chaotic orbit that results from an unfreezing of the Casimir $C = Z_3$ with $\epsilon = 2 \times 10^{-7}$, which then allows the orbit to wander among different leaves (even into the negative C domain). In Fig. 5 (c), $Z_3(t)$

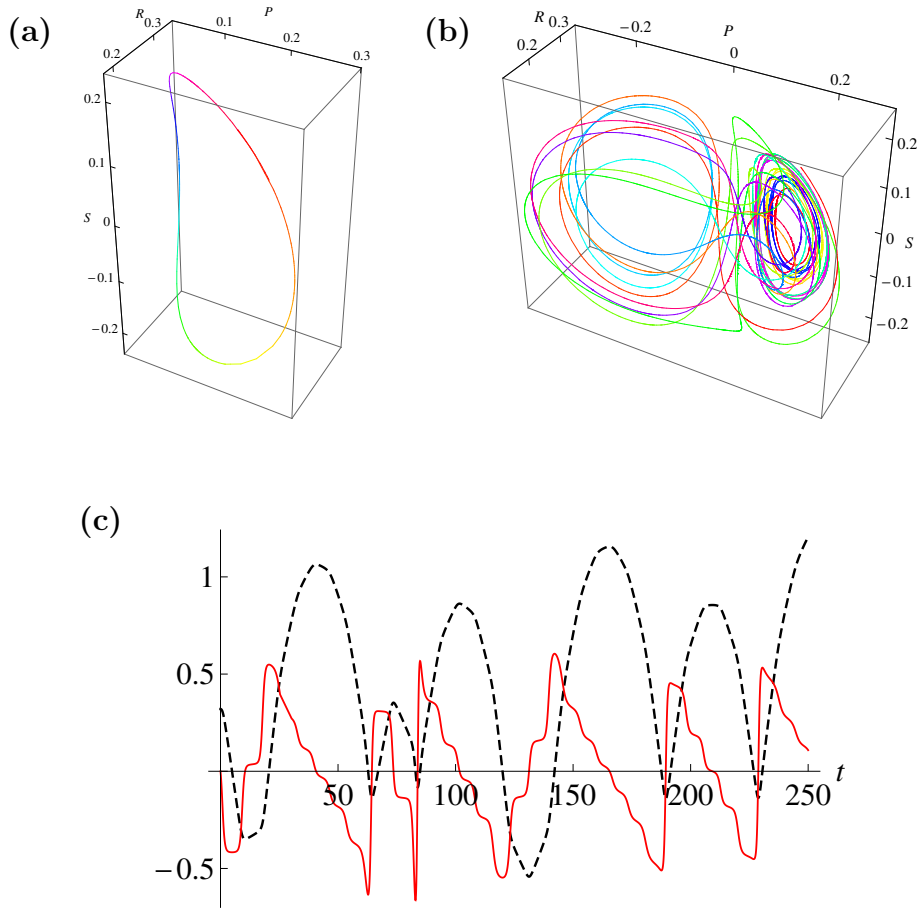


Figure 5. (a) Unperturbed orbit in the $(P R S)$ space. $\lambda = 4, P(0) = R(0) = S(0) = 0.2$. (b) Perturbed chaotic orbit in the $(P R S)$ subspace. $\lambda = 4, P(0) = R(0) = S(0) = 0.2$, and $\epsilon = 2 \times 10^{-7}$. (c) The evolution of $Z_3(t) \times 10^3$ (black dotted) and $Z_4(t) \times 10^{-3}$ (red solid).

is plotted together with its conjugate variable $Z_4(t)$, along with the solution illustrated in (b).

The extended system reveals a variety of phenomena. In Fig. 6, for example, we a solution where the spin reversal (from forward to backward) is accompanied by high-frequency pitching (P); anybody who has done experiments with the rattleback has observed this phenomenon. This happens when the orbit comes close to the S -axis, the singularity of the original Bianchi type $VI_{h \neq -1}$ Poisson matrix, where the Casimir leaves have pronounced skewness (now the variable Z_3 measures the distance from the singularity, which is frozen in the original system as the Casimir invariant). Even after the canonization, the singularity (S -axis) of the original Lie-Poisson algebra remains as a peculiar point around which the dynamics is strongly modified by the singular perturbation (here, the inclusion of the new variable Z_4 works as a singular perturbation, resulting in an increase of the number of degrees of freedom).

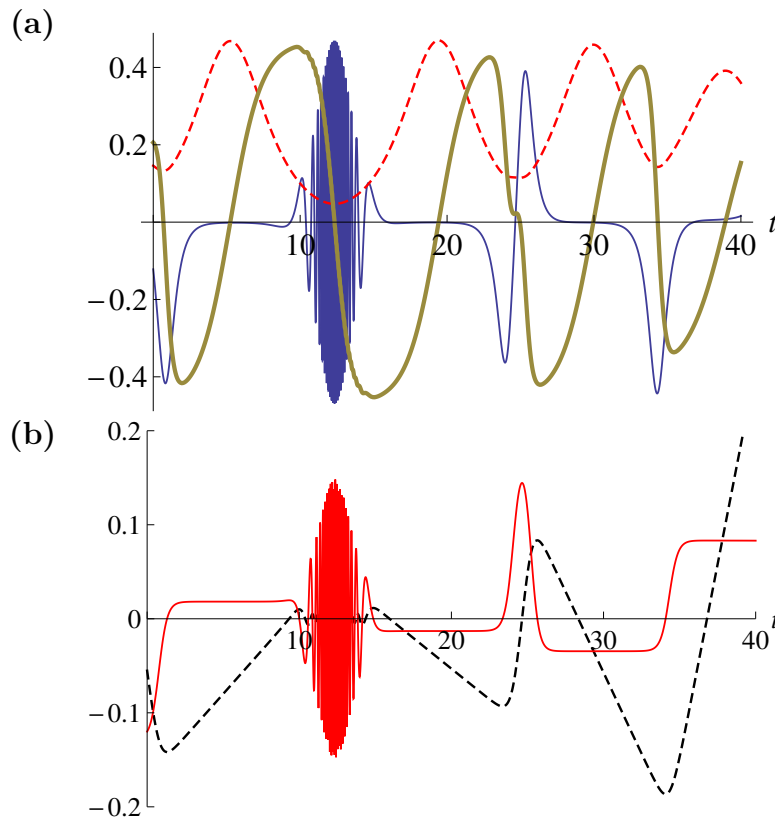


Figure 6. Oscillatory solution; $\lambda = 4$, $P(10) = R(10) = 0.1$, $S(10) = 0.45$ (the initial is given at $t = 10$), and $\epsilon = 10^{-7}$. (a) Plots of $P(t)$ (blue solid), $R(t)$ (red dotted), $S(t)$ (brown thick). (b) Plots of $Z_3(t) \times 10^4$ (black dotted), $Z_4(t) \times 10^{-4}$ (red solid).

5. Conclusion

The rattleback is a rigid body whose ellipsoid of inertia is skewed with respect to the geometry (principal axes) of the contact surface. It is an asymmetric body that moves in a symmetric space, which is the origin of the chirality of the dynamics. However, the curious guiding idea of this paper is that we can reformulate the dynamics as if a symmetric body were moving in an asymmetric space—recall the formalism of section 2, where the Hamiltonian is symmetric but there is something asymmetric in the phase space of the Bianchi type $VI_{h \neq -1}$ Lie-Poisson algebra. The chirality, then, comes from the skewness of the Casimir leaves.

Philosophically, it is interesting to think of the interchangeability of a Hamiltonian and a Casimir as a duality between matter and space. In fact, we can recast the rattle-back equation into an alternative Hamiltonian system with exchanged Casimir and Hamiltonian (see Appendix A). A complex material system may be made simple by transferring complexity to the geometry of space; conversely, a skewed space may be made flat by skewing the matter or the energy. The list of Bianchi algebras (Table 1) provides us with plenty of possibilities for such a transfer.

Acknowledgments

ZY was supported by JSPS KAKENHI Grant Number 23224014, while PJM was supported by the DOE Office of Fusion Energy Sciences, under DE-FG02-04ER-54742.

Appendix A. Dual Hamiltonian formulation

The system (1) has two first integrals, $H = \frac{1}{2}(P^2 + R^2 + S^2)$ and $C = PR^\lambda$. In the Hamiltonian system of section 2, they are the Hamiltonian and a Casimir. We can interchange their roles in a dual Hamiltonian system. Consider the co-symplectic matrix

$$K = \begin{pmatrix} 0 & R^{1-\lambda}S & -R^{2-\lambda} \\ -R^{1-\lambda}S & 0 & PR^{1-\lambda} \\ R^{2-\lambda} & -PR^{1-\lambda} & 0 \end{pmatrix}. \quad (\text{A.1})$$

This time H is a Casimir, while the Hamiltonian C gives the equation of motion (1).

Since K is not linear in \mathbf{X} , the bracket

$$\{F, G\}_K = \langle \partial_{\mathbf{X}}F, K \partial_{\mathbf{X}}G \rangle_{\Omega}$$

is not Lie-Poisson (except in the case $\lambda = 1$, when K is the $\mathfrak{so}(3)$ Lie-Poisson matrix). But there is a nonlinear change of coordinates $\mathbf{X} \mapsto \Xi$ which turns K into an $\mathfrak{so}(3)$ matrix

$$L = \begin{pmatrix} 0 & \Xi_3 & -\Xi_2 \\ -\Xi_3 & 0 & \Xi_1 \\ \Xi_2 & -\Xi_1 & 0 \end{pmatrix}. \quad (\text{A.2})$$

Guided by the common Casimir $H = \frac{1}{2}|\mathbf{X}|^2$ for K and L (classified as Bianchi type IX), we can transform $\mathbf{X} \mapsto \mathbf{Y} \mapsto \Xi$ so that

$$K \mapsto \mathcal{L} = \begin{pmatrix} 0 & 1 & 0 \\ -1 & 0 & 0 \\ 0 & 0 & 0 \end{pmatrix} \mapsto L, \quad (\text{A.3})$$

where the intermediate expression \mathcal{L} is the Darboux normal form; the eigenvector corresponding to the zero eigenvalue is $\partial_{\mathbf{Y}}H$, hence we choose $Y_3 = 2H$ (the factor 2 simplifies formulas later). Since R was what complicated K , we choose $Y_1 = R$. Then the determining condition for Y_2 is

$$\{Y_1, Y_2\}_K = -R^{1-\lambda}S\partial_P Y_2 + PR^{1-\lambda}\partial_S Y_2 = 1,$$

which is readily integrated along the characteristics $P^2 - S^2$ to give $Y_2 = R^{1-\lambda} \arctan(S/P)$. Thus

$$\mathbf{Y} = \begin{pmatrix} R \\ R^{1-\lambda} \arctan(S/P) \\ P^2 + R^2 + S^2 \end{pmatrix}.$$

The transformation $\mathbf{Y} \mapsto \Xi$ is the backtrack of the similar transformation $L \mapsto \mathcal{L}$:

$$\mathbf{Y} = \begin{pmatrix} \Xi_2 \\ \arctan(\Xi_3/\Xi_1) \\ \Xi_1^2 + \Xi_2^2 + \Xi_3^2 \end{pmatrix}.$$

Inverting this relation, we find

$$\Xi = \begin{pmatrix} \sqrt{Y_3 - Y_1^2} \cos Y_2 \\ Y_1 \\ \sqrt{Y_3 - Y_1^2} \sin Y_2 \end{pmatrix} = \begin{pmatrix} \sqrt{P^2 + S^2} \cos[R^{1-\lambda} \arctan(S/P)] \\ R \\ \sqrt{P^2 + S^2} \sin[R^{1-\lambda} \arctan(S/P)] \end{pmatrix}.$$

A direct calculation verifies $L_{12} = \{\Xi_1, \Xi_2\}_K = \Xi_3$, $L_{13} = \{\Xi_1, \Xi_3\}_K = -\Xi_2$, $L_{23} = \{\Xi_2, \Xi_3\}_K = \Xi_1$. Inverting one step further,

$$\mathbf{X} = \begin{pmatrix} P \\ R \\ S \end{pmatrix} = \begin{pmatrix} \pm \sqrt{\Xi_1^2 + \Xi_3^2} / \cos[\Xi_2^{\lambda-1} \arctan(\Xi_3/\Xi_1)] \\ \Xi_2 \\ \pm \sqrt{\Xi_1^2 + \Xi_3^2} / \sin[\Xi_2^{\lambda-1} \arctan(\Xi_3/\Xi_1)] \end{pmatrix}.$$

The Hamiltonian is

$$C = \pm \frac{\Xi_2^\lambda \sqrt{\Xi_1^2 + \Xi_3^2}}{\cos[\Xi_2^{\lambda-1} \arctan(\Xi_3/\Xi_1)]}. \quad (\text{A.4})$$

As noted in Sec. 3.2, chirality is a violation of the symmetry of Hamiltonian spectra, which is possible only with the help of some *singularity*. In the formulation of Sec. 2, the singularity is in the Poisson matrix (so, reflected in the Casimir). In the present *dual* formulation, however, the singularity is transferred to the Hamiltonian (A.4); remember that the present Hamiltonian is the previous Casimir $C = PR^\lambda$.

References

- [1] Moffatt H K and Tokieda T 2008 Celt reversals: a prototype of chiral dynamics, *Proc. Royal Soc. Edinburgh* **138A** 361–368
- [2] Moffatt H K 1978 *Magnetic field generation in electrically conducting fluids* (Cambridge Univ. Press) pp. 212
- [3] Morrison P J 1998 Hamiltonian description of the ideal fluid *Rev. Mod. Phys.* **70** 467–521
- [4] Yoshida Z and Morrison P J 2014 Unfreezing Casimir invariants: singular perturbations giving rise to forbidden instabilities, in *Nonlinear physical systems: spectral analysis, stability and bifurcation*, ed. by O. N. Kirillov and D. E. Pelinovsky (ISTE and John Wiley & Sons), chap. 18, pp. 401–419
- [5] Yoshida Z and Morrison P J 2014 A hierarchy of noncanonical Hamiltonian systems: circulation laws in an extended phase space, *Fluid Dyn. Res.* **46** 031412 (21pp)
- [6] Yoshida Z and Morrison P J 2016 Hierarchical structure of noncanonical Hamiltonian systems, *Phys. Scr.* **91** 024001 (7pp)
- [7] Sudarshan G and Mukunda N 1974 *Classical Dynamics: A Modern Perspective* (Wiley, New York)
- [8] Ellis G F R and MacCallum M A H 1969 A Class of homogeneous cosmological models *Commun. Math. Phys.* **12** 108–141
- [9] Ryan M P and Shepley L C 1975 *Homogeneous Relativistic Cosmologies* *Princeton Ser. Phys.* (Princeton Univ. Press) sec. 6.4
- [10] Meacham S, Morrison P J, and Flierl G 1997 Hamiltonian moment reduction for describing vortices in shear *Phys. Fluids* **9** 2310–2328

- [11] Morrison PJ and Pfirsch D 1989 Free energy expressions for Vlasov equilibria *Phys. Rev. A* **40** 3898–3910
- [12] Morrison PJ and Eliezer S 1986 Spontaneous symmetry breaking and neutral stability in the noncanonical Hamiltonian formalism *Phys. Rev. A* **33** 4205–4214